TOPOSENS

Physics of 3D Ultrasonic Sensors

Nancy Seckel Adi Singh

31 July 2019

---

1. Introduction

Traditional ultrasonic sensors measure one-dimensional distances to only the closest reflecting surface at any given instant. In contrast, 3D ultrasonic sensors – also referred to as 3D sonars – usually have a much wider field-of-view (FoV) and provide simultaneous measurements of multiple objects within their scanning cone. This whitepaper presents the physical principles that govern three-dimensional ultrasonic sensing, with a focus on sonars offered by Toposens.

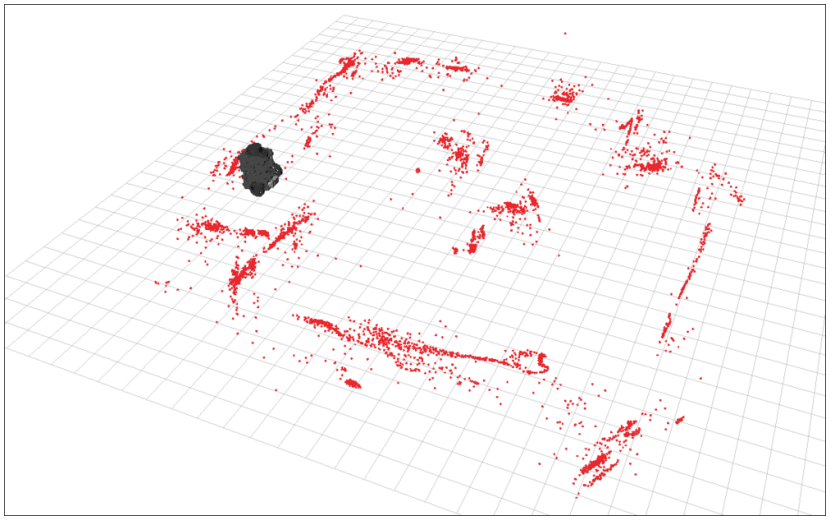

Figure 1: Map of a 2x2 meter arena generated by a TurtleBot using a Toposens sonar.

We hope the content that follows assists readers in understanding the techniques for best utilizing the capabilities of 3D ultrasonic sensors, and in appreciating the limitations of this technology as well. The resulting know-how should enable users to promptly evaluate the suitability of this sensing mode for their planned application.

2. Propagation of Sound Waves

A sound wave consists of pressure changes propagating through a medium with a defined frequency. Molecules in the medium are brought into motion from the vibration of a transmitter, and carry this mechanical, sinusoidal, longitudinal disturbance forward.

Ultrasound refers to such waves with frequencies higher than 20 kHz, which puts them beyond the audible spectrum of humans. The operational range of ultrasonic waves

extends from just a few dozen kilohertz (found in lightweight ranging sensors) to several gigahertz (found in heavy-duty medical imaging devices).

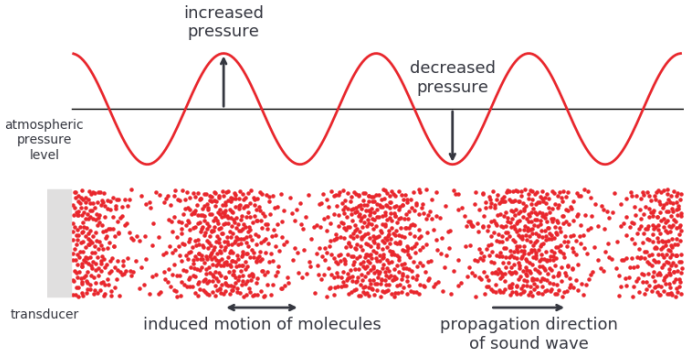

Figure 2: Pressure propagation of a sound wave through air.

3D ultrasonic sonars – like the TS3 from Toposens – transmit ultrasound at a pre-configured frequency and listen for corresponding echoes reflected back from objects in their immediate surroundings. These reflections are captured by an array of on-board microphones and passed to the processor as electrical signals. The processing unit exploits digital signal processing functions that are particularly optimized for its architecture to calculate the spatial location of the echo origin, thus furnishing the 3D coordinates of reflecting objects with respect to the sensor.

This approach, explained in Figure 3, is inspired by echolocation techniques used by bats, dolphins and whales for navigating in the wild (Au & Simmons, 2007).

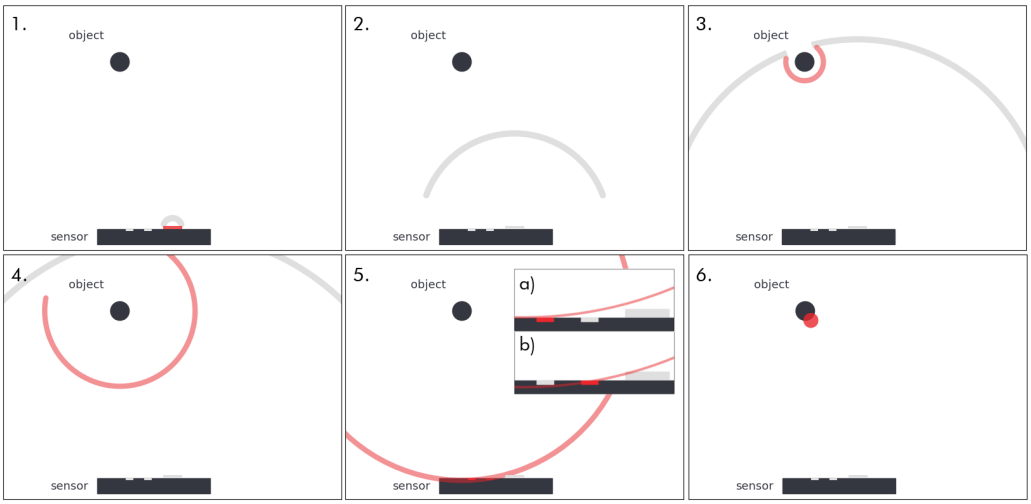

Figure 3: Demonstration of echolocation used in Toposens sonars – [1] the transducer (red) sends out an ultrasound pulse, [2] the wave is carried forward by the air molecules, [3] the wave is reflected by an object, [4] a portion of the echo is directed back to the sensor, [5] the echo is sequentially captured by the microphone array, arriving first at (a) the left microphone, and then at (b) the right microphone, [6] a 3D location of the echo's origin (light red) is determined from the signal's time-of-flight and the delay between microphones receiving the echo.

2.1 Pulsed Emission

To ensure accurate echo localization when utilizing a narrow-band signal, the transducer within the sensor emits short pulses instead of a continuous wave, as shown in Figure 4. This operational mode is referred to as *pulsed ultrasound*. Each pulse contains a specific number of cycles that adds up to the total pulse duration t_p, given by

$$t_p = \frac{n_{cycles}}{f} \tag{1}$$

where f is the frequency of the emitted signal.

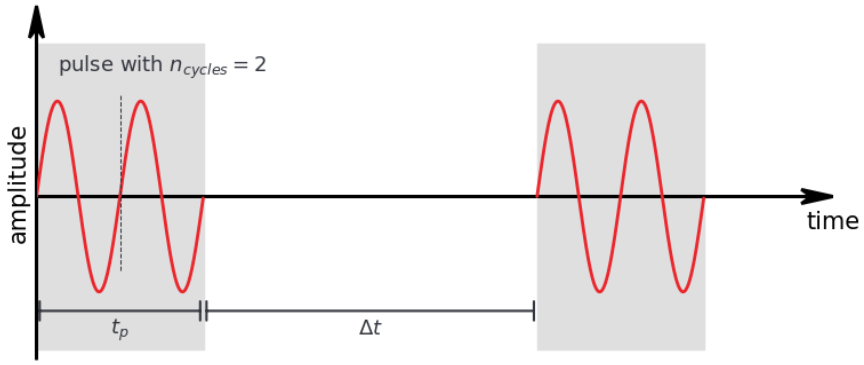

Figure 4: Pulsed emission of a transducer with a waiting period of Δt in between pulses.

To avoid interference of decisive echoes with a subsequent pulse, the sensor waits for a specific duration Δt between consecutive transmissions. This delay should at least exceed the time taken by the wave to reach an object at the maximum scan range r_{max} and travel back to the sensor. Hence,

$$\Delta t \geq \frac{2r_{max}}{c_{air}} \tag{2}$$

where c_{air} is the speed of sound in current environmental conditions. During the waiting period, the sensor's microphones continuously listen for acoustic responses from the environment.

Toposens sensors operate with synchronous calls that do not send out a pulse until all detectable echoes from the previous transmission have been received, parsed and broadcast to the serial port. The number of broadcasts furnished per second by a device is termed as its `scan rate` *in our literature.*

2.2 Attenuation Behavior

As the wave sent out by an ultrasonic sensor travels through air, its intensity diminishes due to scattering, absorption and other mechanisms of energy dispersion. Assuming physical properties of the propagation medium remain constant, this attenuation is

directly proportional to the square of the wave's frequency and exponentially proportional to the distance it traverses.

A consequence of this relationship is that higher frequency sound waves – especially in the ultrasonic spectrum – travel much shorter distances before exhausting all their energy (NDT Resource Center, 2005). Figure 5 shows a qualitative comparison of attenuation characteristics of two signals with different frequencies.

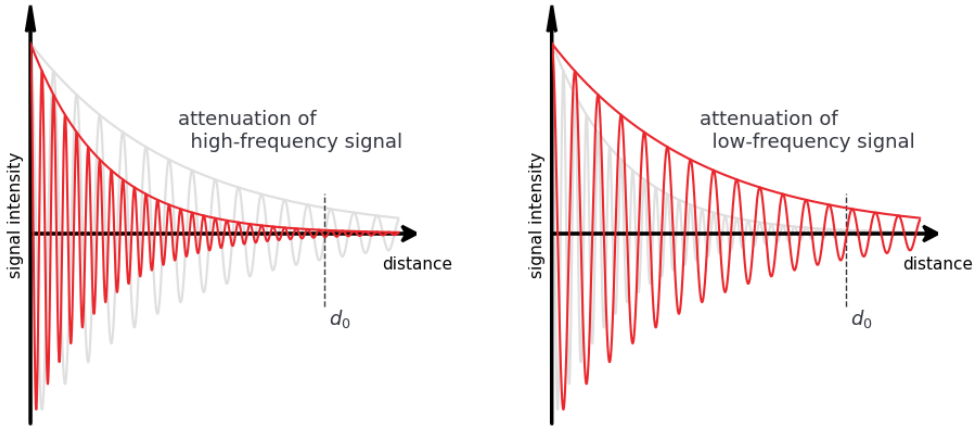

Figure 5: Qualitative attenuation behavior of low- and high-frequency signals. Note that at the same distance d_0 from origin, the first signal's intensity is nearly zero, whereas the second signal still maintains a discernible portion of its intensity.

Toposens devices use a frequency of `41 kHz` to strike a balance between providing reliable measurement data and having a useful scan range of 5 meters. This leads to a wavelength of approximately `8.4 mm` in an indoor environment at 20°C and 30% relative humidity (RH). Objects with an orthogonal surface area smaller than this wavelength induce scattering of the wave, resulting in noisy data in the vicinity of such an object.

2.3 Beam Pattern

The FoV of a ranging device is determined by the `beam pattern` of its transmitters and receivers. In the case of ultrasonic sensors, this beam pattern is the variation of the transducer sound pressure level and microphone sensitivity as a function of direction. It shows the attenuation distribution of the wave and is, therefore, frequency-specific.

The characteristic main lobe of a beam pattern is in the direction of the beam axis at 0°. The presence of additional side lobes at outer angles is also possible. As opposed to 1D ultrasonic sensors, the particular components used in Toposens sonars do not contain side lobes in their beam patterns, and instead present a broad main lobe (Figure 6); effectively allowing sensing in a very wide FoV of up to 160°.

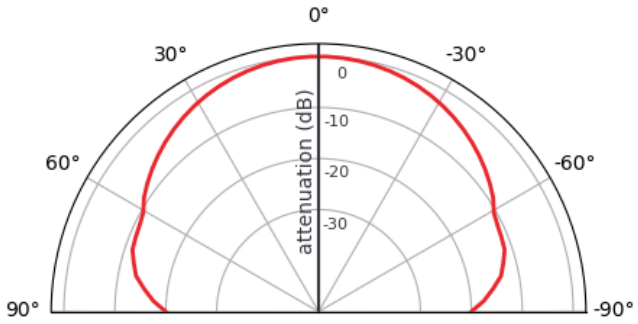

Figure 6: Beam pattern of the transducer used in Toposens TS3 sensors.

3. Calculation of 3D Coordinates

Ultrasonic pulses emitted by a piezoelectric transducer propagate through air and are reflected by surrounding objects. These echoes are received by an array of microphones that convert membrane vibrations into electrical signals, which are subsequently sampled by an analog-to-digital converter (ADC). An example signal envelope of such a response captured in $t_p + \Delta t$ is shown in Figure 4. By measuring the time elapsed between the emitted pulse and a captured response, the range r to an echo's origin can be approximated by

$$r = \frac{c_{air} \cdot t}{2} \tag{3}$$

where t is the elapsed time-of-flight (ToF) for a specific echo.

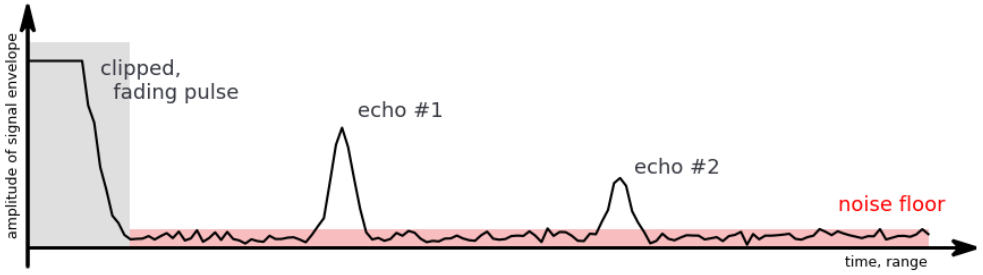

Figure 7: Simplified acoustic response signal for one microphone.

3.1 Angles of Arrival

With this ToF data available, one possible method to determine the echo's angles of arrival – `azimuth` and `elevation` in three-dimensional contexts – is by comparing the relative delay between the different microphones when receiving the same signal response. Determining the Cartesian coordinates from these polar measurements is then a matter of straightforward trigonometric conversion. Note that other methods exist for acquiring more precise angles of arrival and for directly obtaining the 3D Cartesian coordinates of the echo origin. The implementation details of these approaches can be easily found in

academic literature on the topic, for instance, in the works of Steckel, Boen, & Peremans (2012) and Kreczmer (2017).

Toposens uses a proprietary microphone layout to reliably calculate the 3-dimensional origin of each echo. In addition to the 3D coordinates of each echo, the signal strength of each reflection is also tracked. In the pointcloud data stream broadcast by a Toposens sensor, this is labeled as the volume `V` of a detection event.

Since the transducer needs a finite amount of time to stop ringing after sending a pulse, distances of up to 20 cm may present unreliable data. Within this range, the echoes reflecting from objects can interfere with the fading pulse of the last emission. The specifics of this behavior heavily depend on object characteristics and the sensor parameters selected by the user.

3.2 Resolution of Targets

An important characteristic of a sensor that determines distances to multiple objects is its *range resolution*. This is the minimum difference in range needed between two objects for the sensor to distinguish them as separate bodies (Figure 8, left). Below this threshold, the bodies are registered as a single object in the pointcloud (Figure 8, right).

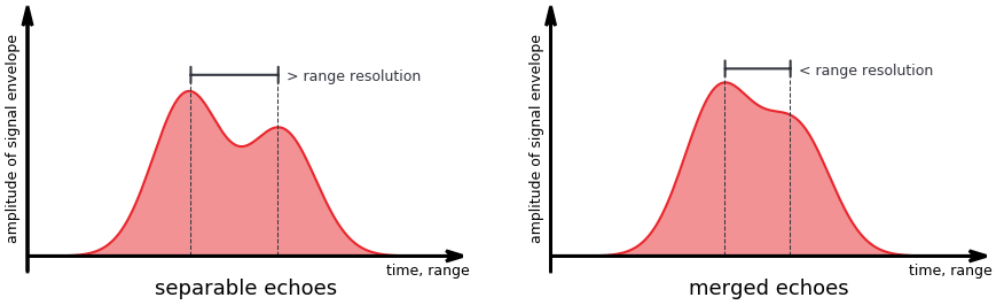

Figure 8: Merging behavior of two echoes in relation to a sensor's range resolution.

Current iterations of Toposens sensors keep the number of microphones to a minimum to reduce latency and ensure real-time processing. Given this constraint, the sensors do not have enough information to guarantee a fixed angular resolution across the full FoV.

A key implication of this trade-off is that echoes from two objects separated by a distance smaller than the sensor's range resolution are not differentiated by the signal processing algorithms. Instead, they appear merged as one point somewhere midway between the two actual point locations depending on the volume of the merging echoes. As a corollary of this, enhancing a device's range resolution would reduce the occurrence of such false merging.

4. Impact of Object Characteristics

Due to the attenuation behavior of waves, objects at farther ranges have to be stronger reflectors for their echoes to be reliably captured by the microphones. The intensity of those echoes is both dependent on an object's material properties as well as its surface structure and geometry.

4.1 Acoustic Impedance Mismatch

Assuming that sound is propagating as a plane wave, the acoustic impedance Z $[kg/m^2s]$ of a material is its average density $[kg/m^3]$ multiplied by the speed of sound $[m/s]$ in it. Waves from in-air sonars are reflected to a larger extent by materials whose acoustic impedance deviates further from that of air (Reddy, Badami, & Balasubramanian, 1994). This is called *impedance mismatch*, and while it is usually large for most solids, there are special foams (Precision Acoustics, 2007) that echo such small portions of the wave that they cannot be picked up by an ultrasonic sensor. The remaining proportion of a wave that is not reflected on the material boundary is further propagating through the medium as can be seen in Figure 9.

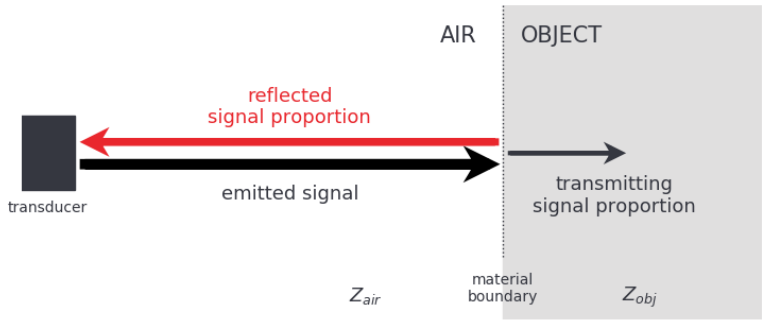

Figure 9: Effect of impedance mismatch on the reflection and transmission of waves at material boundaries.

4.2 Surface Irregularities

As exhibited in Figure 10, reflection occurs in two physical forms, diffuse and specular (Hedrick, 2012). The difference arises from the smoothness of the reflecting surface relative to the wavelength of the incident wave. When the irregularities of an object's surface are smaller than the wavelength of the signal, the wave is reflected in a specular manner; the angle of reflection equaling the angle of incidence.

This condition holds true for most surfaces in man-made environments when using ultrasound at kHz-range frequencies. Waves hitting surfaces with larger irregularities are diffusely reflected in multiple directions, which induces scattering of the signal.

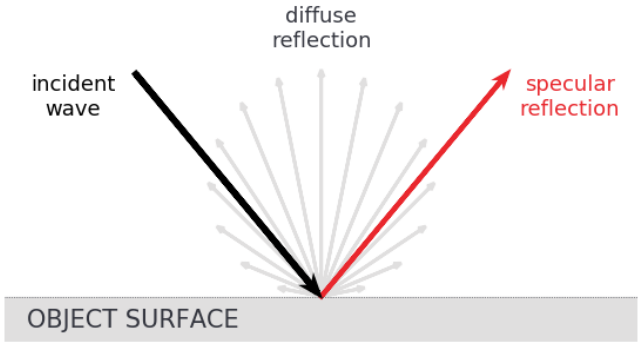

Figure 10: Qualitative visualization of specular and diffuse reflections on an object surface.

This suggests that an echo is predominantly returned to an acoustic sensor by surfaces oriented at an angle of 90°to the incident wave vector. Consequently, all continuous geometries can be detected by the sensor as long as a portion of their surface satisfies the normality condition at the instance of observation.

Rough surfaces are more tolerant to deviations from this condition since their structural aberrations increase the probability of a detectable fraction of the wave being reflected back to the sensor. Smooth surfaces, on the other hand, must be positioned as perpendicular as possible to the sensor for reliable detection.

4.3 Surface Geometry

The 3D coordinates reported by the sensor always correspond to the origin of the strongest reflection in the reported direction. For straight walls, this is the point with the shortest distance to the sensor, that is, the point where the ultrasonic pulse is perpendicularly reflected off the wall. For corners, the ultrasonic pulse might be reflected multiple times before its vector is directed again towards the sensor. In this case, the origin of the strongest echo is located right at the junction of the connected walls (Kleeman & Kuc, 2008).

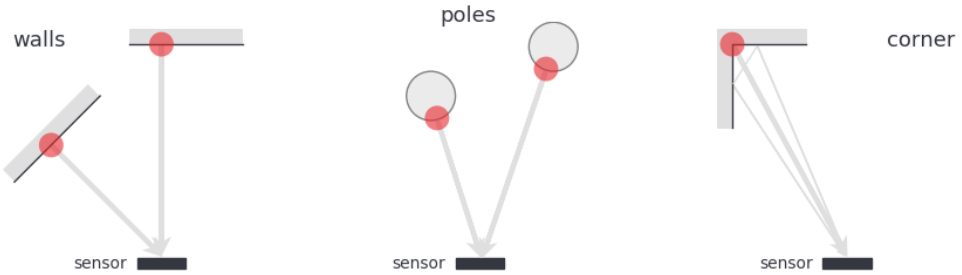

Figure 11: Expected location of 3D points returned for some typical geometries.

The signal strength of the returning echo is further correlated with the size of the surface facing the sensor. For instance, the probability of spotting smaller objects decreases the farther they are placed from the sensor, whereas large planar surfaces like walls can be located up to the maximum scan range r_{max}.

5. Effect of Environment on Measurements

The transmission of ultrasound can be negatively impacted by specific environmental conditions. High levels of dust, humidity, surface temperatures and air flow can increase attenuation of acoustic energy and reduce the typical detection range for specific objects. Furthermore, non-controlled environments can contain other sources of ultrasound – both natural and artificial – that can interfere with object responses and consequently yield inaccurate measurements or even false positives.

5.1 Variations in Speed of Sound

The speed of an ultrasound wave is influenced to varying degrees by physical properties of the propagation medium. For an ideal gas, the speed of sound c_{ideal} is given by the Newton-Laplace equation

$$c_{ideal} = \sqrt{\frac{\gamma \cdot R \cdot 273.15}{M}} \cdot \sqrt{1 + \frac{\theta}{273.15}} \tag{4}$$

where γ is the ratio of the medium's specific heat at constant pressure to that at constant volume, R is the molar gas constant, M is the molar mass of ideal gas and θ is the temperature in °C (Panda, Agrawal, Nshimiyimana, & Hossain, 2016). From this expression we can deduce four physical parameters that affect the speed of sound in air c_{air}:

- temperature
- relative humidity
- changes in atmospheric pressure
- changes in CO_2 concentration

For a given geographical location, variations in pressure due to altitude change and CO_2 concentration are tiny enough to be neglected. In contrast, a change in temperature impacts the speed of sound by roughly 0.18% per degree Celsius (derived from Equation 4), which is a considerable enough deviation that it cannot be ignored. Futhermore, although humidity has a comparatively minor effect on the speed of sound, algorithms running on Toposens sonars account for it to increase measurement accuracy.

Toposens devices allow temperature calibration in two ways: (1) automatically, with their integrated on-board temperature sensor, and (2) manually, with a value provided by the user through the device's command interface. The option to provide custom temperature values enables users to optimize the sonar across different hypothetical temperature scenarios instead of only relying on current ambient conditions.

Calibration for relative humidity is conducted solely via readings from the hygrometric sensor that comes installed on the devices.

5.2 Interference from Other Sources

Though not audible to humans, there can be additional sources of ultrasound within the same frequency band operating around the device. These can interfere with the signals

sent out by the sensor, alter echo amplitudes and create false data points that do not correspond to any real objects.

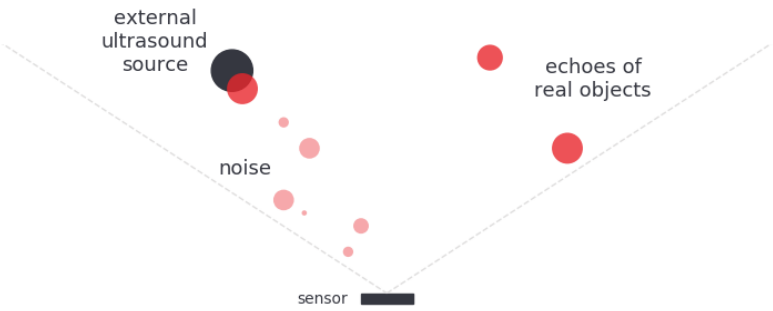

Figure 12: Location of false echoes resulting from external sources of ultrasound.

In case of a single noise source, the origins of these false echoes appear in the direction of the source once processed by the sensor to produce 3D point coordinates (see Figure 12). Once the approximate signature of these false points is experimentally found (given the operational environment and nature of the external source), post-processing filters can be written to remove this noise from the data. Objects with strong reflective properties outside of the noisy region are recognized as usual.

Scan messages returned from Toposens sonars carry a `noise-flag` *in their header-data which indicates the presence of unexpected noise patterns in the received ADC signal or a higher than usual noise floor. The threshold for this flag can be configured by the user for adapting the algorithm's tolerance to ambient noise that satisfies specific application requirements.*

In addition, the devices allow users to explicitly instruct sensors to start and stop sending signals in order to prevent crosstalk in multi-sensor setups. This functionality is demonstrated by the `toposens_sync` *package (Singh, Dengler, & Lang, 2019) developed for the Robot Operating System.*

References

Au, W. W. L., & Simmons, J. A. (2007). Echolocation in dolphins and bats. *Physics Today*, *60*(9), 40. https://doi.org/10.1063/1.2784683

Hedrick, W. R. (2012). *Technology for diagnostic sonography* (pp. 9–13). Elsevier.

Kleeman, L., & Kuc, R. (2008). Sonar sensing. In B. Siciliano & O. Khatib (Eds.), *Springer handbook of robotics* (pp. 491–519). https://doi.org/10.1007/978-3-540-30301-5_22

Kreczmer, B. (2017). Azimuth angle determination for the arrival direction for an ultrasonic echo signal. *Journal of Automation Mobile Robotics and Intelligent Systems*, *11*.

NDT Resource Center. (2005). Attenuation of sound waves. Retrieved from https://www.nde-ed.org/EducationResources/CommunityCollege/Ultrasonics/Physics/attenuation.htm

Panda, K. G., Agrawal, D., Nshimiyimana, A., & Hossain, A. (2016). Effects of environment

on accuracy of ultrasonic sensor operates in millimeter range. *Perspectives in Science*, *8*, 574–576. https://doi.org/10.1016/j.pisc.2016.06.024

Precision Acoustics. (2007). AptFlex f28 technical data sheet. Retrieved from https://www.acoustics.co.uk/pal/wp-content/uploads/2016/05/f28-tds-2019.pdf

Reddy, K. R., Badami, S. B., & Balasubramanian, V. (1994). *Oscillations and waves* (pp. 193–194). Universities Press.

Singh, A., Dengler, S., & Lang, C. (2019). Tools for Prototyping with 3D Ultrasonics in ROS. *Journal of Open Source Software*, *4*(39), 1531. https://doi.org/10.21105/joss.01531

Steckel, J., Boen, A., & Peremans, H. (2012). Broadband 3-d sonar system using a sparse array for indoor navigation. *IEEE Transactions on Robotics*, *29*(1), 161–171.